Chiral *cis*-Platinum Acetylide Complexes via Diphosphine Ligand Exchange: Effect of the Ligand

Amber L. Sadowy, Michael J. Ferguson,[†] Robert McDonald,[†] and Rik R. Tykwinski*

Department of Chemistry, University of Alberta, Edmonton, AB T6G 2G2, Canada

Received July 5, 2008

Chiral, bidentate phosphine ligands (*R,R*-CHIRAPHOS, *R*-PROPHOS, *S,S*-BDPP, *R,R*-Me-DUPHOS, *R,R*-NORPHOS) react with *trans*-platinum acetylide complexes **1a** and **1b**, $(Ph_3P)_2Pt(C{\equiv}CR)_2$ (R = TIPS, *p*-MeC_6H_4), via ligand exchange to generate chiral platinum acetylide complexes. The corresponding *cis*-platinum complexes are formed in all cases except for the reaction of **1b** with *S,S*-BDPP, where the dimeric complex **4d′** is the product. Conversely, the reaction of **1a** and **1b** with the ligands *S,S*-DIOP, *R*-BINAP, and *R*-SYNPHOS fails to give the desired product in appreciable yield. Circular dichroism spectroscopy is used to examine the effect of the chiral ligand on the chiroptical properties of the platinum acetylide framework. X-ray crystallographic analyses of achiral complex **1a** and chiral derivative **4e** are reported.

Introduction

Platinum acetylide complexes (e.g., **1a** and **1b**, Scheme 1) can be easily formed via a number of methods, often through the simple reaction of a terminal acetylene with $(R_3P)_2PtCl_2$.[1,2] In addition to small-molecule complexes, these versatile alkynylation reactions have been exploited for the formation of carbon-rich oligomers,[3] polymers,[4] macrocycles,[5] and supramolecular assemblies.[6] Furthermore, the reductive elimination of platinum from *cis*-complexes to generate butadiynes has been established, expanding the usefulness of these compounds.[7]

It has been shown that when PPh_3 is present as the ligands, *trans*-acetylides **1** can be transformed smoothly into the corresponding *cis*-acetylides (e.g, **3** or **4**, Scheme 1) via ligand exchange with *cis*-bis(diphenylphosphino)ethylene (dppee, **2a**, Figure 1).[8] This ligand exchange protocol has also been successfully used with *R,R*- or *S,S*-CHIROPHOS (**2b**) to generate chiral products, including a number of macrocycles.[9,10] In the present study, the prospect of forming chiral acetylide complexes via ligand exchange has been explored for two series

Scheme 1. Ligand Exchange Reaction with *trans*-Platinum Acetylides 1a,b

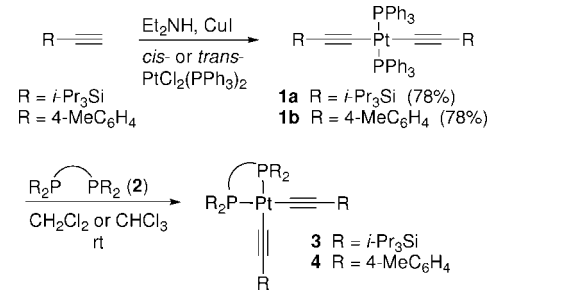

* Corresponding author. E-mail: rik.tykwinski@ualberta.ca.
[†] X-ray Crystallography Laboratory, University of Alberta.

(1) (a) Sonogashira, K.; Fujikura, Y.; Yatake, T.; Toyoshima, N.; Takahashi, S.; Hagihara, N. *J. Organomet. Chem.* **1978**, *145*, 101–108. (b) Sonogashira, K.; Yatake, T.; Tohda, Y.; Takahashi, S.; Hagihara, N. *J. Chem. Soc., Chem. Commun.* **1977**, 291–292. (c) Nelson, J. H.; Jonassen, H. B.; Roundhill, D. M. *Inorg. Chem.* **1969**, *8*, 2591–2596.

(2) Reviews, see: (a) Lee, S. J.; Lin, W. *Acc. Chem. Res.* **2008**, *41*, 521–537. (b) Yam, V. W. W.; Tao, C. H. In *Carbon-Rich Compounds*; Haley, M. M., Tykwinski, R. R. Eds.; Wiley-VCH, 2006; Chapter 10. (c) Kaiser, A.; Bäuerle, P. *Top. Curr. Chem.* **2005**, *249*, 127–201. (d) Long, N. J.; Williams, C. K. *Angew. Chem., Int. Ed.* **2003**, *42*, 2586–2617. (e) Takahashi, S.; Onitsuka, K.; Takei, F. *Macromol. Symp.* **2000**, *156*, 69–77. (f) Yam, V. W.-W. *Acc. Chem. Res.* **2002**, *35*, 555–563. (g) Youngs, W. J.; Tessier, C. A.; Bradshaw, J. D. *Chem. Rev.* **1999**, *99*, 3153–3180.

(3) (a) Stahl, J.; Mohr, W.; de Quadras, L.; Peters, T. B.; Bohling, J. C.; Martín-Alvarez, J. M.; Owen, G. R.; Hampel, F.; Gladysz, J. A. *J. Am. Chem. Soc.* **2007**, *129*, 8282–8295. (b) de Quadras, L.; Bauer, E. B.; Mohr, W.; Bohling, J. C.; Peters, T. B.; Martín-Alvarez, J. M.; Hampel, F.; Gladysz, J. A. *J. Am. Chem. Soc.* **2007**, *129*, 8296–8309. (c) Cardolaccia, T.; Funston, A. M.; Kose, M. E.; Keller, J. M.; Miller, J. R.; Schanze, K. S. *J. Phys. Chem. B* **2007**, *111*, 10871–10880. (d) Seneclauze, J. B.; Retailleau, P.; Ziessel, R. *New J. Chem.* **2007**, *31*, 1412–1416. (e) Long, N. J.; Wong, C. K.; White, A. J. P. *Organometallics* **2006**, *25*, 2525–2532. (f) Jones, S. C.; Coropceanu, V.; Barlow, S.; Kinnibrugh, T.; Timofeeva, T.; Brédas, J.-L.; Marder, S. R. *J. Am. Chem. Soc.* **2004**, *126*, 11782–11783. (g) Liu, Y.; Jiang, S.; Glusac, K.; Powell, D. H.; Anderson, D. F.; Schanze, K. S. *J. Am. Chem. Soc.* **2002**, *124*, 12412–12413. (h) Siemsen, P.; Gubler, U.; Bosshard, C.; Günter, P.; Diederich, F. *Chem.−Eur. J.* **2001**, *7*, 1333–1341. (i) Leininger, S.; Stang, P. J.; Huang, S. *Organometallics* **1998**, *17*, 3981–3987.

(4) (a) Zhou, G.-J.; Wong, W.-Y.; Ye, C.; Lin, Z. *Adv. Funct. Mater.* **2007**, *17*, 963–975. (b) Khan, M. S.; Al-Mandhary, M. R. A.; Al-Suti, M. K.; Corcoran, T. C.; Al-Mahrooqi, Y.; Attfield, J. P.; Feeder, N.; David, W. I. F.; Shankland, K.; Friend, R. H.; Köhler, A.; Marseglia, E. A.; Tedesco, E.; Tang, C. C.; Raithby, P. R.; Collings, J. C.; Roscoe, K. P.; Batsanov, A. S.; Stimson, L. M.; Marder, T. B. *New J. Chem.* **2003**, *27*, 140–149. (c) Chawdhury, N.; Köhler, A.; Friend, R. H.; Younus, M.; Long, N. J.; Raithby, P. R.; Lewis, J. *Macromolecules* **1998**, *31*, 722–727. (d) Takahashi, S.; Kariya, M.; Yatake, T.; Sonogashira, K.; Hagaihara, N. *Macromolecules* **1978**, *11*, 1063–1166.

(5) (a) Hua, F.; Kinayyigit, S.; Rachford, A. A.; Shikhova, E. A.; Goeb, S.; Cable, J. R.; Adams, C. J.; Kirschbaum, K.; Pinkerton, A. A.; Castellano, F. N. *Inorg. Chem.* **2007**, *46*, 8771–8783. (b) Johnson, C. A., II; Baker, B. A.; Berryman, O. B.; Zakharov, L. N.; O'Connor, M. J.; Haley, M. M. *J. Organomet. Chem.* **2006**, *691*, 413–421. (c) Campbell, K.; McDonald, R.; Ferguson, M. J.; Tykwinski, R. R. *Organometallics* **2003**, *22*, 1353–1355. (d) Bosch, E.; Barnes, C. L. *Organometallics* **2000**, *19*, 5522–5524. (e) Faust, R.; Diederich, F.; Gramlich, V.; Seiler, P. *Chem.−Eur. J.* **1995**, *1*, 111–117. (f) ALQaisi, S. M.; Galat, K. J.; Chai, M.; Ray, D. G., III; Rinaldi, P. L.; Tessier, C. A.; Youngs, W. J. *J. Am. Chem. Soc.* **1998**, *120*, 12149–12150.

(6) (a) Cardolaccia, T.; Li, Y. J.; Schanze, K. S. *J. Am. Chem. Soc.* **2008**, *130*, 2535–2545. (b) Bäuerle, P.; Ammann, M.; Wilde, M.; Götz, G.; Mena-Osteritz, E.; Rang, A.; Schalley, C. A. *Angew. Chem., Int. Ed.* **2007**, *46*, 363–368. (c) Hasegawa, T.; Furusho, Y.; Katagiri, H.; Yashima, E. *Angew. Chem., Int. Ed.* **2007**, *46*, 5885–5888. (d) Campbell, K.; Ooms, K. J.; Wasylishen, R. E.; Tykwinski, R. R. *Org. Lett.* **2005**, *7*, 3397–3400. (e) Onitsuka, K.; Fujimoto, M.; Kitajima, H.; Ohshiro, N.; Takei, F.; Takahashi, S. *Chem.−Eur. J.* **2004**, *10*, 6433–6446.

10.1021/om800633h CCC: $40.75
Publication on Web 11/07/2008

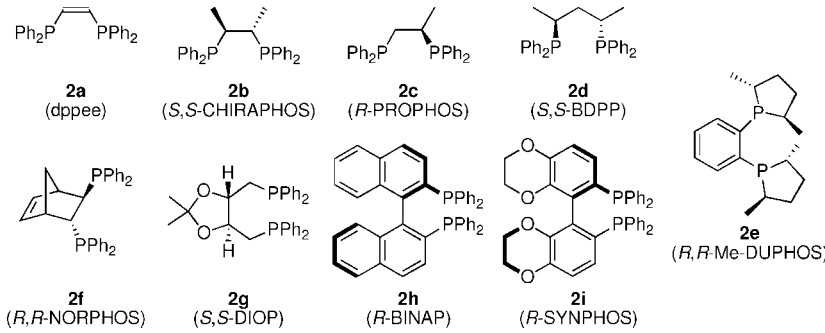

Figure 1. Diphosphine ligands **2a**−**i**.

of *trans*-acetylide precursors, **1a** and **1b**, using a greatly expanded range of chiral bidentate phosphine ligands **2b**−**i**. Changes in the CD spectra of the products **3** and **4** are then used to empirically assay the affect of the various chiral ligands. The results of this investigation are presented herein.

Results and Discussion

Compounds **1a**[8] and **1b** are readily available via the reaction of either triisopropylsilyl- or *p*-tolylacetylene with *trans*-$(PPh_3)_2PtCl_2$ (Scheme 1).[11] Because the *trans*-isomer of **1** is thermodynamically more stable than the corresponding *cis*-isomer, the room-temperature reaction of the precursor acetylene with *cis*-$(Ph_3P)_2PtCl_2$ also forms exclusively the *trans*-complex. The analogous reaction of a terminal acetylene with *trans*-$(PEt_3)_2PtCl_2$ is also possible, but attempts to effect ligand exchange with the resulting PEt_3 complexes of **1** have not been successful. Thus, compounds **1a** and **1b**, with PPh_3, have been utilized for the current study, even though their solubility in common organic compounds is much reduced versus those with PEt_3 ligands.

Ligand exchange reactions of **1a** and **1b** with chelating diphosphines **2a**−**i** (Figure 1) were explored by adding 1 equiv of the appropriate ligand to a solution of either **1a** or **1b** in CH_2Cl_2 (CD_2Cl_2) or $CHCl_3$ ($CDCl_3$). Using ligands **2a**−**f** (Table 1), the reactions typically proceeded quickly at room temperature (hours) and could be easily monitored by thin-layer chromatography or ^{31}P NMR spectroscopy. The ^{31}P NMR spectra clearly showed the disappearance of the signal of **1a** and **1b** at δ 21 ($^1J_{P-Pt}$ = 2728 Hz) and δ 19.7 ($^1J_{P-Pt}$ = 2660 Hz), respectively, and the appearance of a new signal of the *cis*-product. The $^1J_{P-Pt}$ coupling constants were particularly diagnostic for confirming ligand exchange: they shifted from 2500−2800 Hz for the *trans*-acetylides **1a**,**b** to ∼2100−2300 Hz for *cis*-acetylide products. All complexes could be readily purified via column chromatography, using either silica gel (**3a**−**f**) or alumina (**4a**−**f**).

The reaction of *trans*-Pt-acetylide complex **1a** with *S*,*S*-DIOP (**2g**) resulted in a mixture of unidentified products based on the ^{31}P NMR spectrum. Surprisingly, the reaction of **1a** with *R*-BINAP (**2h**) and *R*-SYNPHOS (**2i**) did not result in ligand exchange, even after heating and extended reaction times. The ^{31}P NMR spectra of these latter two reactions showed only signals of *trans*-Pt-acetylide complex **1a** and the free ligand *R*-BINAP (**2h**) or *R*-SYNPHOS (**2i**).

Table 1. Synthesis of *cis*-Pt-Acetylides 3 and 4 via Ligand Exchange

precursor	ligand **2**	pdct	yield [%]
1a	**2a** (dppee)	**3a**	95
1a	**2b** (*R*,*R*-CHIRAPHOS)	**3b**	85
1a	**2c** (*R*-PROPHOS)	**3c**	81
1a	**2d** (*S*,*S*-BDPP)	**3d**	68
1a	**2e** (*R*,*R*-Me-DUPHOS)	**3e**	88
1a	**2f** (*R*,*R*-NORPHOS)	**3f**	90
1b	**2a** (dppee)	**4a**	48
1b	**2b** (*R*,*R*-CHIRAPHOS)	**4b**	49
1b	**2c** (*R*-PROPHOS)	**4c**	83
1b	**2d** (*S*,*S*-BDPP)	**4d′**	44[a]
1b	**2e** (*R*,*R*-Me-DUPHOS)	**4e**	81
1b	**2f** (*R*,*R*-NORPHOS)	**4f**	72

[a] See text for discussion.

The product of the reaction of **1b** with *S*,*S*-BDPP (**2d**) deserves special comment. The ^{31}P NMR spectrum of the product isolated from this reaction revealed a signal at 26.9 ppm for the two equivalent phosphine atoms and showed an anomalous coupling constant of $^1J_{P-Pt}$ = 2585 Hz, i.e., one that was more characteristic of a *trans*-Pt-acetylide complex. Furthermore, the ESI mass spectral analysis of this product (in the presence of AgOTf) showed a strong signal at *m*/*z* 1837 corresponding to $[2M + Ag]^+$. These observations indicate that the expected *cis*-Pt-acetylide depicted in Scheme 1 is not the likely product, but, rather, a dimeric Pt-containing complex was formed with two bridging *S*,*S*-BDPP ligands, **4d′** (Figure 2). The analogous dimeric species was not observed in the synthesis of *S*,*S*-BDPP complex **3d**, likely due to the greater steric demands of the bulky TIPS groups in comparison to the planar tolyl group. A similar bundling effect has been observed by Gladysz and co-workers, using platinum-endcapped polyynes in reactions with the achiral 1,3-diphosphine ligand $Ph_2P(CH_2)_3PPh_2$ to give the dimers **5** (Figure 2).[12] In the case of the triyne derivative **5** (n = 3), X-ray crystallographic analysis of three different crystalline solvates was used to confirm the structure of this species.

All *cis*-Pt-acetylide complexes **3a**−**f** and **4a**−**f** have been fully characterized by ^1H, ^{31}P, and ^{13}C NMR and IR spectroscopies, mass spectral analysis, and microanalysis when possible. The ^{31}P NMR spectra were particularly informative, with signal(s) in the range 5−66 ppm and $^1J_{P-Pt}$ coupling constants in the expected range 2100−2300 Hz (with the exception of **4d′**, vide

(7) (a) Furusho, Y.; Tanaka, Y.; Yashima, E. *Org. Lett.* **2006**, *8*, 2583–2586. (b) Fuhrmann, G.; Debaerdemaeker, T.; Bäuerle, P. *Chem. Commun.* **2003**, 948–949. (c) James, S. L.; Younus, M.; Raithby, P. R.; Lewis, J. *J. Organomet. Chem.* **1997**, *543*, 233–235.

(8) Campbell, K.; McDonald, R.; Ferguson, M. J.; Tykwinski, R. R. *J. Organomet. Chem.* **2003**, *683*, 379–387.

(9) Campbell, K.; Johnson, C. A., II; McDonald, R.; Ferguson, M. J.; Haley, M. M.; Tykwinski, R. R. *Angew. Chem., Int. Ed.* **2004**, *43*, 5967–5971.

(10) For other examples of ligand exchange at a Pt-acetylide center, see refs 3a and 7a.

(11) See Supporting Information for details.

(12) Owen, G. R.; Hampel, F.; Gladysz, J. A. *Organometallics* **2004**, *23*, 5893–5895.

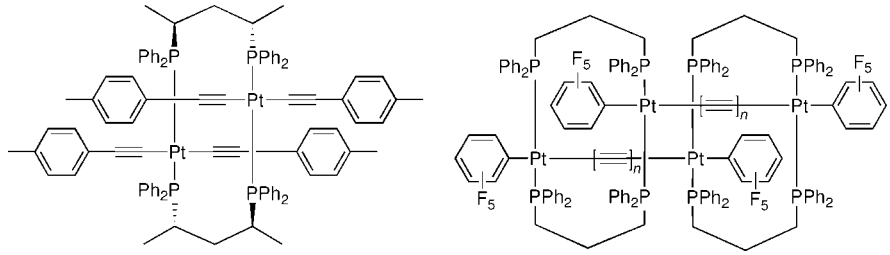

Figure 2. Dimeric Pt-acetylide complex **4d′** formed with two bridging *S*,*S*-BDPP ligands and dimers **5** synthesized by Gladysz and coworkers.

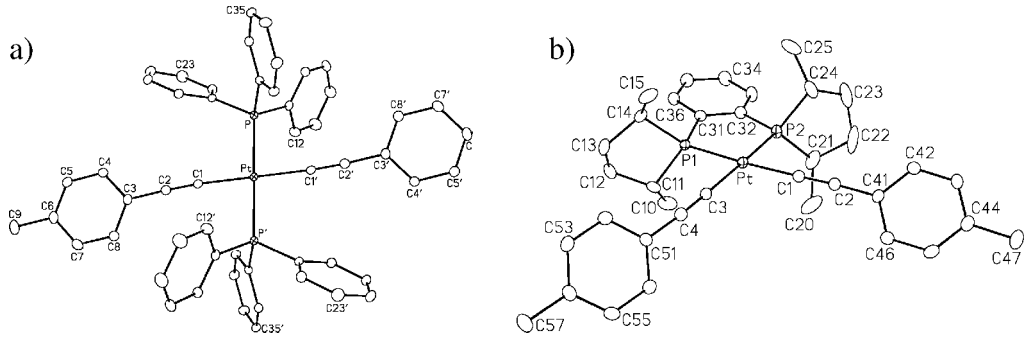

Figure 3. ORTEP drawings of (a) compound **1b** (20% probability level). Selected bond lengths (Å): Pt−C(1) 2.021(4), C(1)−C(2) 1.192(5), Pt−P 2.2862(10). Selected bond angles (deg): C(1)−Pt−C(1)′ 180.0(2), C(1)−Pt−P 93.95(11), C(1)−Pt−P′ 86.05(11), P−Pt−P′ 180.0. (b) Compound **4e** (20% probability level, cocrystallized solvent molecule, CH_2Cl_2, not shown). Selected bond lengths (Å): Pt−C(1) 2.014(4), Pt−C(3) 2.035(4), C(1)−C(2) 1.209(5), C(3)−C(4) 1.187(6), Pt−P(1) 2.2571(10), Pt−P(2) 2.2513(10). Selected bond angles (deg): C(1)−Pt−C(3) 93.86(14), C(1)−Pt−P(2) 89.74(11), C(3)−Pt−P(1) 89.66(10), P(1)−Pt−P(2) 86.78(4).

infra). The ^{13}C NMR spectroscopic analysis of the *cis*-Pt-acetylide complexes proved to be challenging due to the complex splitting pattern caused by the magnetically nonequivalent phosphorus atoms and platinum coupling. The analysis was significantly more complicated for the *R*-PROPHOS- and *R*,*R*-NORPHOS-containing compounds **3c**, **3f**, **4c**, and **4f**, where the phosphorus atoms are not chemical shift equivalent. Nevertheless, the discussion of several assignments is useful. For complexes **3a**−**f** the α-acetylide ($L_2Pt(C{\equiv}CR)_2$) carbon signal has a chemical shift of 122−129 ppm, while for complexes **4a**−**f** it appears upfield in the range 101−112 ppm (in $CDCl_3$). This resonance is typically observed as a doublet of doublets (dd), with coupling constants $^2J_{C-P}(trans)$ = 133−169 Hz and $^2J_{C-P}(cis)$ = 4−48 Hz. Without an excellent signal-to-noise ratio, $^1J_{C-Pt}$ for the α-acetylide carbon is not usually observed.[13] The β-acetylide carbon ($L_2Pt(C{\equiv}CR)_2$) is observed for the *cis*-complexes in the range 103−112 ppm with $^3J_{C-P}(trans)$ = 3−35 Hz and $^3J_{C-P}(cis)$ < 5 Hz (not always observed).[14] With sufficient signal-to-noise, coupling constants $^2J_{C-Pt}$ = 229−307 Hz are also observed for the β-acetylide carbon.

The solid-state structural properties of *trans*-complex **1b** and *R*,*R*-Me-DUPHOS complex **4e** have been examined by X-ray crystallographic analysis (Figure 3, Table 2). Single crystals of **1b** suitable for crystallographic analysis were grown by the slow diffusion of Et_2O into a CH_2Cl_2 solution at 4 °C. Crystals of **4e** were grown by slow evaporation of a CH_2Cl_2/acetone solution at room temperature. As a result of its centrosymmetric structure, the ≡C−Pt−C≡ and P−Pt−P bond angles of **1b** are linear at 180°. A slight deviation from overall square-planar geometry about the Pt center is, however, observed with C(1)−Pt−P and C(1)−Pt−P′ bond angles of 93.95(11)° and 86.05(11)°, respectively. The geometry about Pt in **4e** also deviates slightly from square planar, with a ≡C−Pt−C≡ bond angle of 93.86(14)° and a P(1)−Pt−P(2) bond angle of 86.78(4)°.[15] The C(1)−Pt−P(2) and C(3)−Pt−P(1) bond angles are nearly identical at 89.74(11)°

Table 2. X-Ray Crystallographic Details for 1b and 4e

	1b	**4e**
formula	$C_{54}H_{44}P_2Pt$	$C_{36}H_{42}P_2Pt{\bullet}CH_2Cl_2$
fw	949.92	816.65
cryst size, mm	0.27 × 0.14 × 0.04	0.60 × 0.48 × 0.27
cryst syst	monoclinic	orthorhombic
space group	$P2_1/n$ (No. 14)	$P2_12_12_1$ (No. 19)
a, Å	13.6022(8)	9.8524(9)
b, Å	8.5341(5)	18.9860(18)
c, Å	18.0885(11)	19.5240(18)
β, deg	90.4470(10)	
V, Å^3	2099.7(2)	3652.1(6)
Z	2	4
D_{calc}, g cm^{-3}	1.502	1.485
T, K	193	193
2θ limit, deg	52.76	52.80
μ, mm^{-1}	3.455	4.099
total data	15 514	28 887
no indep reflns	4274	7450
no reflns $F_o^2 \geq 2\sigma F_o^2$	3258	7206
no. params	260	391
restraints	0	3[a]
goodness of fit	1.102	1.091
$R(F)$ [$F_o^2 \geq 2\sigma(F_o^2)$]	0.0250	0.0203
wR_2 [$F_o^2 \geq -3\sigma(F_o^2)$]	0.0736	0.0573
lgst diff peak and hole, e Å^{-3}	0.955 and −0.412	1.069 and −0.771
CCDC no.	679334	679335

[a] Distances within the two sets of atomic positions for the disordered solvent dichloromethane molecule were constrained to be equal (within 0.001 Å).

(13) To confirm this signal assignment, a $^{13}C\{^1H, ^{31}P\}$ NMR spectrum for **4e** was recorded with sufficient signal-to-noise that this coupling was clearly discernible, providing $^1J_{C-Pt}$ = 1105 Hz. See Supporting Information (Figures S45−47).

(14) Compound **4c** does not follow this trend, with observed coupling constants for the alpha acetylenic carbon of $^2J_{C-P}$ = 85 and 86 Hz (*trans*) and $^2J_{C-P}$ = 3.0 and 2.7 Hz (*cis*).

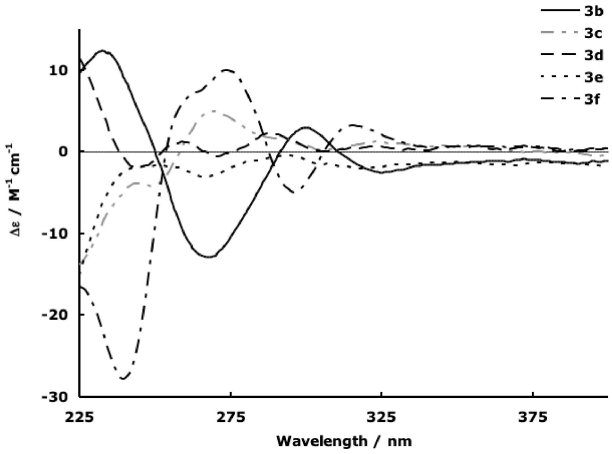

Figure 4. Circular dichroism spectra of compounds **3b**−**f** in CH_2Cl_2.

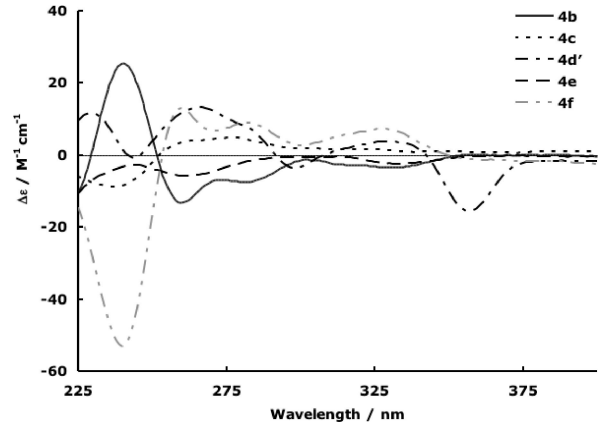

Figure 5. Circular dichroism spectra of compounds **4b**−**f** in CH_2Cl_2.

and 89.66(10)°, respectively. When comparing bond lengths between the *trans*- and *cis*-Pt-acetylide complexes **1b** and **4e**, the only noteworthy difference is found for the Pt−P bonds where the *cis*-Pt−acetylide bonds of **4e** are slightly shorter (by ca. 0.03 Å).

The electronic absorption characteristics of acetylide complexes **3b**−**f** and **4b**−**f** were examined by UV−vis and CD spectroscopies.[16] The *cis*-Pt-acetylide complexes **3b**−**f** all have two absorption maxima in their UV−vis spectra; the lower energy absorption is observed between 293 and 301 nm and attributed to the MLCT absorption.[17] The higher energy absorption is observed between 257 and 268 nm, ascribed to a $\pi-\pi^*$ transition of the ligands. In the CD spectra, only the *S*,*S*-CHIRAPHOS- and *R*,*R*-NORPHOS-containing compounds **3b** and **3f** show any remarkable features (Figure 4). Both have a weak, low-energy band at 291 and 288 nm, respectively, and a strong, high-energy bisignate band at 254 and 253 nm, respectively. Complexes **3c**−**e** either do not contain a bisignate band (**3e**) or display only a weak signal in the higher energy region (**3c** and **3d**). The *R*,*R*-NORPHOS-containing compound **3f** has the most intense signal in the CD spectrum of $\Delta\varepsilon = 28$ M^{-1} cm^{-1} (240 nm), and the *S*,*S*-CHIRAPHOS-containing compound **3b** has the second largest signal of $\Delta\varepsilon = 13$ M^{-1} cm^{-1} (268 nm).

Similar to complexes **3b**−**f**, tolyl derivatives **4b**, **4c**, **4e**, and **4f** all have two absorption maxima in their UV−vis spectra. The lower energy absorption is observed between 317 and 325 nm and is attributed to the MLCT absorption, while the higher energy absorption observed between 257 and 263 nm is presumably due to the $\pi-\pi^*$ transition for ligands. None of the complexes have a significant signal in their CD spectra that appears to correspond to the lower energy absorption (Figure 5), and only the *R*,*R*-Me-DUPHOS compound **4e** *does not* contain a bisignate band corresponding to the higher energy absorption. These bisignate signals are centered at 252, 252, and 253 nm for compounds **4b**, **4c**, and **4f**, respectively. The *R*,*R*-NORPHOS compound **4f** shows the strongest signal at $\Delta\varepsilon = -53$ M^{-1} cm^{-1} (240 nm), followed by **4b** (*S*,*S*-CHIRAPHOS, $\Delta\varepsilon = 25$ M^{-1} cm^{-1} at 241 nm).

In summary, it is clear from the CD spectra that the magnitude of $\Delta\varepsilon$ is dependent on the chiral ligand present in the complex, ranging from nearly zero to 53 M^{-1} cm^{-1}. Consistently, *R*,*R*-NORPHOS (**2f**) produced the most substantial $\Delta\varepsilon$ values, followed by *S*,*S*-CHIRAPHOS (**2b**). Ligands *R*-PROPHOS (**2c**) and *R*,*R*-Me-DUPHOS (**2e**) provided little or no effect. While still empirical, these comparisons do suggest that *R*,*R*-NORPHOS and *S*,*S*-CHIRAPHOS are most effective in providing for chirality transfer from the diphosphine ligand to the framework of the platinum acetylide complexes studied. This outlines a valuable design principle toward the construction of larger and functional chiral molecules based on platinum acetylide building blocks.

Experimental Section

Reagents were purchased reagent grade from commercial suppliers and used without further purification. THF was distilled from sodium/benzophenone ketyl; hexanes and CH_2Cl_2 were distilled from CaH_2 immediately prior to use. Compounds **1a**, **3a**, and **3b** were prepared as previously reported.[8,9] Column chromatography was carried out on aluminum oxide (neutral, Brockman 1, 150 mesh) from Aldrich Chemical Co., Inc. or silica gel-60 (230−400 mesh) from General Intermediates of Canada or Silicycle. Thin-layer chromatography (TLC) was done on aluminum sheets coated with aluminum oxide 60 F_{254} from EM Separations or plastic sheets coated with silica gel G UV_{254} from Macherey-Nagel and visualized by UV light. IR spectra were done with a Nic-Plan IR Microscope on films cast from CH_2Cl_2. For IR data, useful functional groups and 3−4 of the strongest absorptions are reported including, but not limited to, C−H, C═C, and C≡C bond stretches. ^1H, ^{13}C, and ^{31}P NMR spectra were acquired on a Varian-400 at 27 °C in either $CDCl_3$ or CD_2Cl_2. Solvent peaks 7.24, 5.32 for ^1H and 77.00, 53.80

(15) For a discussion of the significance of P−Pt−P bite angles, see for example: (a) Freixa, Z.; van Leeuwen, P. W. N. M. *Dalton Trans.* **2003**, 1890–1901. (b) van Leeuwen, P. W. N. M.; Kamer, P. C. J.; Reek, J. N. H.; Dierkes, P. *Chem. Rev.* **2000**, *100*, 2741–2769. (c) Casey, C. P.; Whiteker, G. T. *Isr. J. Chem.* **1990**, *30*, 299–304.

(16) The UV−vis spectra were recorded for pure ligands **2b**−**f**, and all show a high-energy absorption between 254 and 263 nm corresponding to the $\pi-\pi^*$ transition for the phenyl chromophores with $\varepsilon < 16\,000$ M^{-1} cm^{-1}. These absorptions are also present in all of the *cis*-Pt-acetylide complexes that contain these ligands. The circular dichroism (CD) spectral analysis of the pure ligands *R*-PROPHOS (**2c**) and *S*, *S*-BDPP (**2d**) show weak signals at 228 and 243 nm, respectively, while the CD spectra of *S*,*S*-CHIRAPHOS (**2b**), *R*,*R*-Me-DUPHOS (**2e**), and *R*,*R*-NORPHOS (**2f**) contain stronger signals at 229, 317, and 233 nm, respectively. The CD spectra of all five ligands show at least one cross-over point in the range 236−275 nm. In all cases the absolute signal intensity of the pure ligand is $\Delta\varepsilon < 10$ M^{-1} cm^{-1} for absorptions ≥225 nm; see Supporting Information for spectra (Figures S1 and S2).

(17) For discussion of MLCT in Pt-acetylides, see: (a) Ref 2e. (b) Saha, R.; Qaium, M. A.; Debnath, D.; Younus, M.; Chawdhury, N.; Sultana, N.; Kociok-Köhn, G.; Ooi, L.-L.; Raithby, P. R.; Kijima, M. *Dalton Trans.* **2005**, *2760*, 2765. (c) D'Amato, R.; Furlani, A.; Colapietro, M.; Portalone, G.; Casalboni, M.; Falconieri, M.; Russo, M. V. *J. Organomet. Chem.* **2001**, *627*, 13–22. (d) Khan, M. S.; Kakkar, A. K.; Long, N. J.; Lewis, J.; Raithby, P.; Nguyen, P.; Marder, T. B.; Wittmann, F.; Friend, R. H. *J. Mater. Chem.* **1994**, *4*, 1227–1232.

for ^{13}C, respectively, were used as reference and H_3PO_4 as ^{31}P reference. For simplicity, the coupling constants of the aryl protons for *para*-substituted tolyl groups have been reported as pseudo-first-order, even though they are second-order (AA′XX′) spin systems. Coupling constants *J* are reported as observed. EI-MS (70 eV) were done with a Kratos MS 50 instrument, and ESI-MS with either a Micromass Zabspec oaTOF or PE Biosystems Mariner TOF instrument. For mass spectral analyses, low-resolution data are provided in cases when M^+ is not the base peak; otherwise, only high-resolution data are provided. Elemental analyses were performed by the Microanalytical Service, Department of Chemistry, University of Alberta. Circular dichroism spectra were recorded at 20.0 °C, from 550 to 220 nm with 330 increments, on an OLIS DSM 17 CD, Cary-17 Conversion spectrometer/circular dichroism module, Online Instruments Inc., with a 1 mm (Hellma) cuvette. UV−vis spectra were acquired with a Varian Cary 400 Scan spectrometer at room temperature with a 1 cm quartz cuvette. The same solutions used for CD spectroscopy were used for UV−vis spectroscopy, and the appropriate dilutions were prepared to result in UV absorbencies in the range of $A = 0.2-4.0$. The CD and UV−vis spectra were recorded the same day for each sample. To ensure the data were statistically equivalent, the standard deviation of three replicates was calculated and any results >10% were discarded. The raw data of the replicates were then averaged to produce a single spectrum.[18]

Representative Procedures. *cis*-(*R*,*R*-Me-DUPHOS)Pt(C≡C−Si*i*-Pr$_3$)$_2$ (3e). 1,2-Bis[(2*R*,5*R*)-2,5-dimethylphospholano]benzene (**2e**, 8.9 mg, 0.029 mmol) was added to a solution of **1a** (31 mg, 0.029 mmol) in dry CH_2Cl_2 (5 mL). The mixture was stirred at rt for 48 h. Solvent removal and purification via gradient column chromatography (silica gel, CH_2Cl_2/hexanes (1:2) to CH_2Cl_2/hexanes (1:1)) afforded **3e** (22 mg, 88%) as a white solid: mp 193−197 °C; $R_f = 0.72$ (CH_2Cl_2/hexanes, 2:1); UV−vis (CH_2Cl_2) λ_{max} (ϵ) 268 (13 600), 301 (11 000) nm; IR (CH_2Cl_2, cast) 2938, 2860 cm^{-1}; ^1H NMR (400 MHz, $CDCl_3$) δ 7.67−7.63 (m, 2H), 7.56−7.52 (m, 2H), 3.50−3.38 (m, 2H), 2.74−2.61 (m, 2H), 2.36−2.16 (m, 6H), 1.73−1.62 (m, 2H), 1.48 (d, $J = 7.0$ Hz, 3H), 1.44 (d, $J = 7.0$ Hz, 3H), 1.12 (d, $J = 3.0$ Hz, 18H), 1.11 (d, $J = 2.9$ Hz, 18H), 1.08−0.99 (m, 6H), 0.86 (d, $J = 7.2$ Hz, 3H), 0.83 (d, $J = 7.2$ Hz, 3H); $^{13}C\{^1H\}$ NMR (100 MHz, $CDCl_3$) δ 143.8 (pseudo-t, $J_{C-P} = 36$ Hz), 132.8 (pseudo-t, $J_{C-P} = 8.2$ Hz), 130.9 (br), 128.9 (dd, $^2J_{C-P} = 133$ Hz (*trans*), $^2J_{C-P} = 14$ Hz (*cis*)), 109.2 (d, $^3J_{C-P} = 29$ Hz (*trans*)), 40.8 (d, $J_{C-P} = 34$ Hz), 37.3−36.4 (m), 36.1, 19.04, 19.02, 17.7−17.3 (m), 14.1, 12.0; $^{31}P\{^1H\}$ NMR (162 MHz, $CDCl_3$) δ 65.3 (pseudo-t, $^1J_{P-Pt} = 2134$ Hz); ESI-HRMS ($ClCH_2CH_2Cl$) calcd for $C_{40}H_{71}P_2PtSi_2$ ($[M + H]^+$) 864.4217, found 864.4220.

***cis*-(*R*,*R*-Me-DUPHOS)Pt(C≡C-*p*-CH$_3$-C$_6$H$_4$)$_2$ (4e).** 1,2-Bis-[(2*R*,5*R*)-2,5-dimethylphospholano]benzene (**2e**, 8.3 mg, 0.027 mmol) was added to a solution of **1b** (26 mg, 0.027 mmol) in dry CH_2Cl_2 (10 mL). The mixture was stirred at rt for 16 h. Solvent removal and purification via column chromatography (alumina, hexanes) afforded **4e** (16 mg, 81%) as a yellow solid: mp 199 °C (dec); $R_f = 0.44$ (CH_2Cl_2/hexanes, 2:1); UV−vis (CH_2Cl_2) λ_{max} (ϵ) 263 (40 900), 325 (16 900) nm; IR (CH_2Cl_2, cast) 2923, 2108, 1504 cm^{-1}; ^1H NMR (400 MHz, $CDCl_3$) δ 7.72−7.67 (m, 2H), 7.60−7.57 (m, 2H), 7.35 (d, $J = 8.1$ Hz, 4H), 7.02 (d, $J = 8.4$, 4H), 3.54−3.38 (m, 2H), 2.81−2.71 (m, 2H), 2.40−2.23 (m, 4H), 2.30 (s, 6H), 2.15−2.05 (m, 2H), 1.76−1.65 (m, 2H), 1.54 (d, $J = 7.0$ Hz, 3H), 1.49 (d, $J = 7.0$ Hz, 3H), 0.88 (d, $J = 7.2$ Hz, 3H), 0.84 (d, $J = 7.2$ Hz, 3H); $^{13}C\{^1H\}$ NMR (100 MHz, $CDCl_3$) δ 143.6 (pseudo-t, $J_{C-P} = 36$ Hz), 134.6, 132.8 (pseudo-t, $J_{C-P} = 8.3$ Hz), 131.2 (br), 128.3, 125.4, 111.9 (d, $^3J_{C-P} = 35$ Hz (*trans*)), 106.3 (dd, $^2J_{C-P} = 143$ Hz (*trans*), $^2J_{C-P} = 15$ Hz (*cis*)), 40.5 (d, $J_{C-P} = 34$ Hz), 37.5−36.9 (m), 36.3 (br), 21.2, 17.5 (pseudo-t, $J_{C-P} = 3.5$ Hz), 13.9; $^{31}P\{^1H\}$ NMR (162 MHz, $CDCl_3$) δ 66.4 (pseudo-t, $^1J_{P-Pt} = 2206$ Hz); EIMS *m*/*z* 731.2 (M^+, 70), 501.1 ($[M - 2(C\equiv C\text{-}p\text{-Me-}C_6H_4)]^+$, 100); HRMS calcd for $C_{36}H_{42}P_2Pt$ (M^+) 731.2410, found 731.2419.

Acknowledgment. This work has been generously supported by the University of Alberta and the Natural Sciences and Engineering Research Council of Canada (NSERC) through the Discovery Grant program. The authors thank the staff, in particular Wayne Moffat, of the Analytical and Instrumentation Laboratory at the University of Alberta, for their help with the circular dichroism spectroscopy.

Supporting Information Available: Complete experimental procedures; spectroscopic data for all new compounds; NMR, CD, and UV−vis spectra of new compounds; crystallographic information for **1b** and **4e** in CIF format. This material is available free of charge via the Internet at http://pubs.acs.org.

OM800633H

(18) For a detailed description of the procedure used for the UV−vis and CD spectroscopic studies, see the Supporting Information.